The Astrophysical Journal Letters, 797:L30 (5pp), 2014 December 20 doi:10.1088/2041-8205/797/2/L30

LABORATORY FORMATION OF FULLERENES FROM PAHS: TOP-DOWN INTERSTELLAR CHEMISTRY

Junfeng Zhen[1,2], Pablo Castellanos[1,2], Daniel M. Paardekooper[2],
Harold Linnartz[2], and Alexander G. G. M. Tielens[1]
[1] Leiden Observatory, Leiden University, P.O. Box 9513, 2300-RA Leiden, The Netherlands; zhen@strw.leidenuniv.nl
[2] Sackler Laboratory for Astrophysics, Leiden Observatory, Leiden University, P.O. Box 9513, 2300-RA Leiden, The Netherlands
Received 2014 October 29; accepted 2014 November 21; published 2014 December 9

ABSTRACT

Interstellar molecules are thought to build up in the shielded environment of molecular clouds or in the envelope of evolved stars. This follows many sequential reaction steps of atoms and simple molecules in the gas phase and/or on (icy) grain surfaces. However, these chemical routes are highly inefficient for larger species in the tenuous environment of space as many steps are involved and, indeed, models fail to explain the observed high abundances. This is definitely the case for the C_{60} fullerene, recently identified as one of the most complex molecules in the interstellar medium. Observations have shown that, in some photodissociation regions, its abundance increases close to strong UV-sources. In this Letter we report laboratory findings in which C_{60} formation can be explained by characterizing the photochemical evolution of large polycyclic aromatic hydrocarbons (PAHs). Sequential H losses lead to fully dehydrogenated PAHs and subsequent losses of C_2 units convert graphene into cages. Our results present for the first time experimental evidence that PAHs in excess of 60 C-atoms efficiently photo-isomerize to buckminsterfullerene, C_{60}. These laboratory studies also attest to the importance of top-down synthesis routes for chemical complexity in space.

Key words: astrochemistry – ISM: molecules – methods: laboratory: molecular – molecular processes – photon-dominated region (PDR)

Online-only material: color figures

1. INTRODUCTION

Over the last 80 yr, observational studies have revealed the presence of ∼180 different molecules in space (Herbst & van Dishoeck 2009; Tielens 2013). Because of intrinsic limitations the observational techniques, the molecular inventory revealed by these studies is heavily biased toward small polar species, radicals, and linear carbon chains with electronegative groups (e.g., CN). Also larger (6–10 atoms containing) stable molecules like methanol and ethylene glycol have been identified (Herbst & van Dishoeck 2009). With the advent of infrared space missions, a richer and diverse molecular universe was brought to light (Tielens 2008, and references therein). Most mid-infrared spectra are dominated by broad features at 3.3, 6.2, 7.7, 8.6 and 11.2 μm, generally attributed to IR fluorescence of UV-pumped, large (50–100 C-atoms) polycyclic aromatic hydrocarbon (PAHs) molecules (Tielens 2008, and references therein). These molecules contain ∼10% of the elemental carbon and play an important role in the ionization and energy balance of the interstellar medium (ISM) of galaxies. Recently, in addition to these PAH bands, the infrared signatures of buckminsterfullerene, C_{60}, were also observed at 7.0, 8.5, 17.4 and 18.9 μm (Cami et al. 2010; Sellgren et al. 2010). PAH bands are also prominent in planet-forming disks around young stars (Habart et al. 2006; Doucet et al. 2007) and PAHs as well as C_{60} are important components of solar system meteorites (Sephton & Botta 2008; Becker et al. 1994). Hence, understanding the processes that regulate the origin and evolution of these species and their relationship to the organic inventory of space has become a focus in astrochemistry.

In the tenuous ISM, direct synthesis of PAHs and fullerenes from small hydrocarbon species is inhibited (McEwan et al. 1999) and PAHs are generally thought to form in the C-rich ejecta of asymptotic giant branch stars as molecular intermediaries or byproducts of the soot formation process (Frenklach & Feigelson 1989; Cherchneff et al. 1992). In the ISM, these species are then processed by ultraviolet photons, which leads initially to their ionization. Subsequently, UV photolysis results in dissociation, and sequential steps of double H-losses, have been identified as the dominant fragmentation channel, leading to pure carbon clusters, likely in the form of graphene sheets (Ekern et al. 1998; Joblin 2003; Berné & Tielens 2012; Zhen et al. 2014). After complete dehydrogenation, ongoing photolysis will break down the carbon skeleton leading to smaller carbon species. It has been suggested that highly excited graphene sheets may also isomerize to more stable carbon cages or fullerenes (Berné & Tielens 2012). Rapid transformation of graphene flakes into the C_{60} fullerene is observed in electron irradiation experiments of graphene on surfaces (Chuvilin et al. 2010). Fullerenes also fragment in a strong UV field through the loss of C_2 units, shrinking the size of the cage until the smallest photostable fullerene, C_{32}, is reached (Handschuh et al. 1995). From this point on, fragmentation leads to the formation of rings and chains (Lifshitz 2000).

Photodissociation regions (PDRs) provide a natural laboratory for the study of the interaction of UV photons with carbonaceous species (Pety et al. 2005; Rapacioli et al. 2005; Hollenbach & Tielens 1999). Observations with the *Spitzer Space Telescope* and the *Herschel Space Observatory* of the prototypical PDR, NGC 7023, have revealed that the C_{60} abundance increases by an order of magnitude while the PAH abundance decreases when approaching the illuminating star (Berné & Tielens 2012). These observations point toward the important role of photochemistry in the destruction of interstellar PAHs and that C_{60} is likely a photochemical product of PAHs (Berné & Tielens 2012; Castellanos et al. 2014). So far, experimental evidence of this process has been lacking.

In this Letter, we present laboratory results demonstrating the formation of fullerenes (in particular C_{60}) from large PAHs by photolysis, based on the difference in absorption properties as a function of wavelength (Tatsuhisa et al. 1991). We compare and contrast the fragmentation pattern of fullerenes (C_{60} and C_{70}) to that of PAHs and their fragmentation products. As the C_{60} fullerene does not absorb at 532 nm, while PAHs and other fullerenes absorb efficiently, the absorption behavior of C_{60} fragments produced by photolysis of PAHs can be used to establish the presence of C_{60} fullerenes.

2. EXPERIMENTAL METHODS

We have studied the fragmentation of fully benzenoid PAH cations and fullerene cations in the laboratory using i-PoP, our instrument for photodissociation of PAHs, which is described in detail in Zhen et al. (2014). Briefly, PAHs or fullerenes are sublimated in an oven, at an appropriate temperature, ionized by an electron gun, and transported into a quadrupole ion-trap via an ion gate. Later, the cations are irradiated by many (typically ~18) pulses from a nanosecond pulsed Nd:YAG laser, leading to sequential steps of fragmentation. The ion-trap content is subsequently released and analyzed using a reflectron time-of-flight mass spectrometer. Each fragmentation step is initiated by absorption of multiple photons; the exact number depends on the laser wavelength. The process is heavily biased toward dissociation through the lowest energy channel (Zhen et al. 2014).

Here, we study the photo-fragmentation behavior of the large PAH cations $C_{60}H_{22}^{+}$ (m/z = 742.172), $C_{66}H_{26}^{+}$ (m/z = 818.203), and $C_{78}H_{26}^{+}$ (m/z = 962.203). The mass spectra are contrasted with those resulting from photo-fragmentation of the fullerene cations C_{60}^{+} (m/z = 720) and C_{70}^{+} (m/z = 840), in order to investigate the formation of C_{60} from large PAHs. These particular PAHs are selected because their armchair edges provide them with greater stability than PAHs with zigzag edges (Poater et al. 2007; Koskinen et al. 2008), which may favor their presence in space. Indeed, PAHs with armchair edges are observed to be more abundant in regions close to strong UV sources (Candian et al. 2014).

3. RESULTS

Studies at our laboratory and elsewhere have shown that, for small PAHs, several fragmentation channels are available (e.g., H loss, C_2H_2 loss; Jochims et al. 1994). However, for large PAHs, fragmentation is almost exclusively through sequential hydrogen loss (Ekern et al. 1998; Joblin 2003; Zhen et al. 2014). As an example, the dehydrogenation of $C_{66}H_{26}^{+}$ the hydrogenation state moves progressively toward fully dehydrogenated species (Figure 1). At even higher laser powers, these pure carbon molecules and the fullerenes fragment through the loss of C_2 units (Figure 2), as has been observed in other studies (Lifshitz 2000).

Fullerene formation in graphite vaporization experiments routinely gives rise to "magic numbers" of C-atoms (60, 56, 50, 44) with enhanced abundances compared to neighboring peaks, reflecting their greater stability (Zimmerman et al. 1991). We can use this pattern as an indication of the formation of fullerene structures in our photofragmentation studies. Panels A and B in Figure 2 show the fragmentation through C_2 losses experienced by C_{60}^{+}, $C_{60}H_{22}^{+}$, $C_{66}H_{26}^{+}$ and C_{70}^{+} at 266 nm and 355 nm, respectively. We observe that, in both cases, the fullerene "magic number" mass peaks show an enhanced intensity with respect

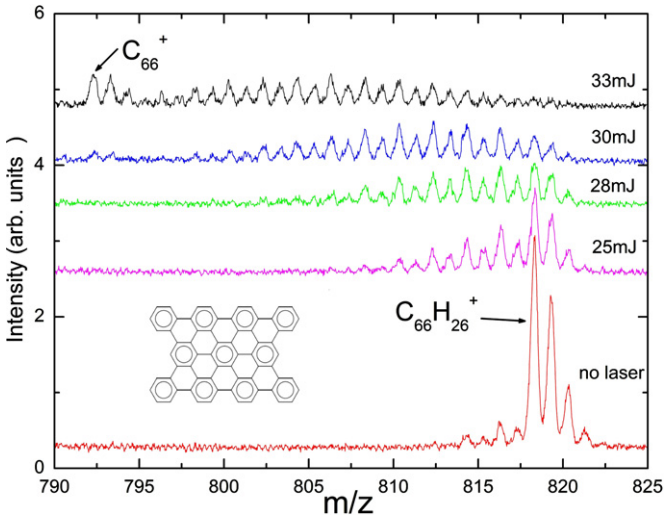

Figure 1. Fragmentation pattern of the fully benzenoid cation, $C_{66}H_{26}^{+}$, irradiated at 355 nm as a function of laser power. Additional peaks in the no-laser trace are isotopes and fragmentation produced by the electron gun.

(A color version of this figure is available in the online journal.)

to neighboring peaks irrespective of the parent molecule except for the C_{60}^{+} fragment from $C_{60}H_{22}^{+}$, where the enhancement is minimal when compared to that of the other parent molecules. The differences observed between the two wavelengths are due to variations in laser power—at shorter wavelengths, the laser system has a limited power output—, which is particularly clear for the PAHs, where the smallest fragments are not produced at 266 nm.

Figure 3 shows the C-losses for the same species at 532 nm. In this case the dissociation behavior of the fullerenes and PAHs is markedly different. For the fullerenes, the dissociation stops when reaching clusters with 60 C-atoms (in the case of C_{60}^{+} no dissociation is observed). The PAHs considered here experience fragmentation up to much smaller masses. However, there is a striking difference in the behavior of the C_{60}^{+} peak. For $C_{60}H_{22}^{+}$ this peak does not appear to be special when compared to those further down the line, while in the case of $C_{66}H_{26}^{+}$ it shows a clear enhancement and remains even when all neighboring peaks have practically disappeared.

The kinetics of the fragmentation process is controlled by the absorption properties of the parent species and its daughter products, and by the dissociation energy of the fragmentation channels involved. The dependence on absorption properties provides a tool with which the fragmentation products can be probed. The PAH cations and the fullerenes C_{60}^{+} and C_{70}^{+} as well as their products absorb well at 266 and 355 nm (Tatsuhisa et al. 1991; Malloci et al. 2007). However, C_{60}^{+} does not absorb at 532 nm (Tatsuhisa et al. 1991) and does not fragment, even at very high laser powers (Figure 3). For C_{70}^{+}, it is clear that C_{60}^{+} is formed, thus halting the fragmentation at 532 nm. The fragmentation pattern of $C_{60}H_{22}^{+}$ is not indicative for a hard to dissociate 60 C-atom cluster, ruling out formation of significant amounts of buckminsterfullerene. Fragmentation of the pure carbon cluster produced from $C_{66}H_{26}^{+}$ can be represented by a combination of the behavior of the fullerene C_{70}^{+} and that of the $C_{60}H_{22}^{+}$ PAH cation, indicating formation of the C_{60} fullerene.

The formation of fullerenes from large PAHs may be a more general process. The fragmentation pattern observed for

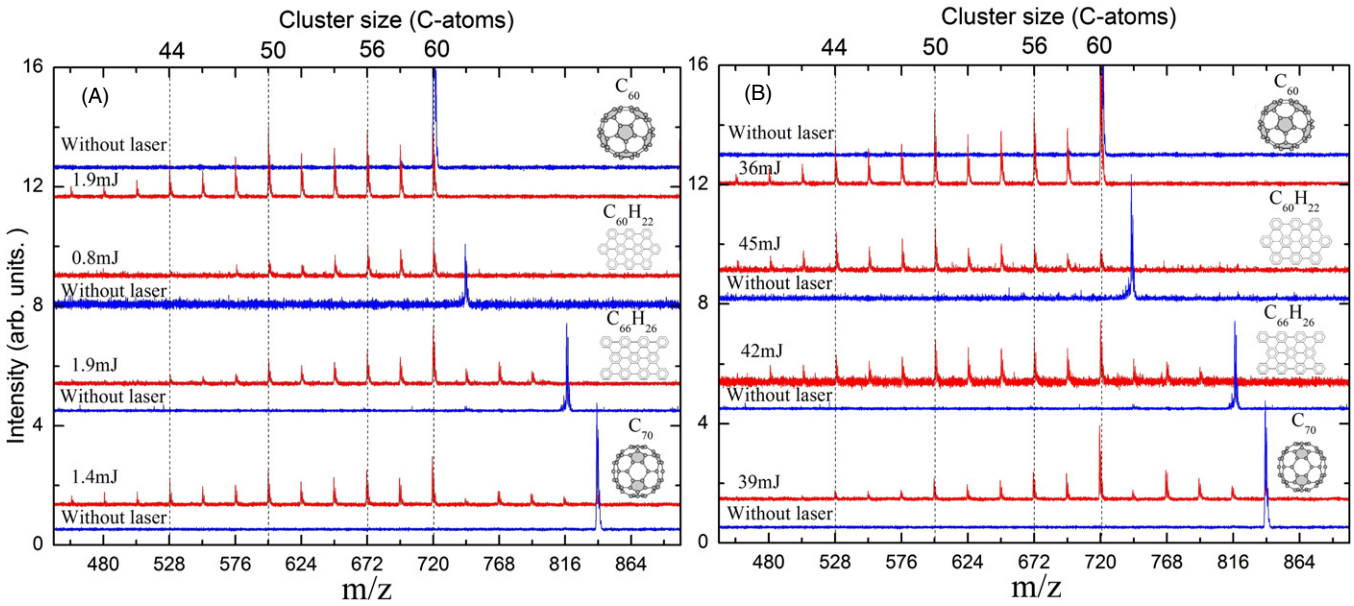

Figure 2. Comparison of the fragmentation pattern of the fully benzenoid cations, $C_{60}H_{22}^{+}$ and $C_{66}H_{26}^{+}$, and the fullerene cations, C_{60}^{+} and C_{70}^{+}, irradiated at 266 (panel (A)) and 355 nm (panel (B)). Note that the fragmentation pattern of the PAHs resembles that of the fullerenes. The "magic numbers" are marked by the vertical dashed lines and correspond to peaks with an m/z of 720 for C_{60}^{+}, 672 for C_{56}^{+}, 600 for C_{50}^{+} and 528 for C_{44}^{+}.

(A color version of this figure is available in the online journal.)

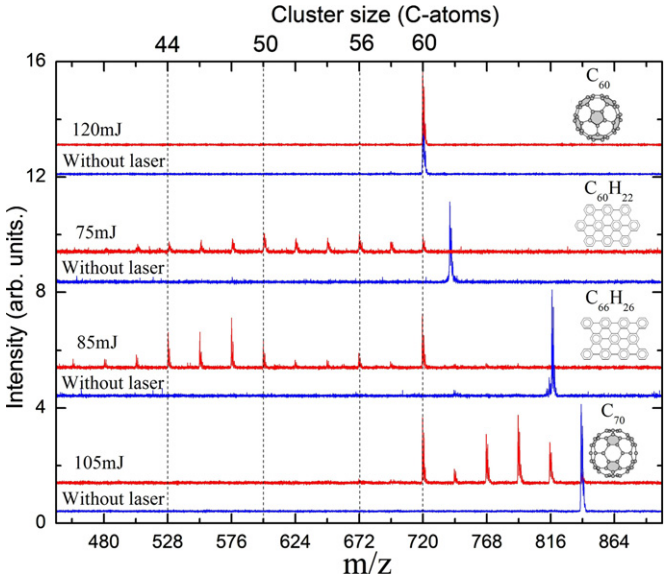

Figure 3. Comparison of the fragmentation pattern of the molecules considered in Figure 2, irradiated at 532 nm. At this wavelength, the fullerene C_{60}^{+} cation does not absorb and no fragmentation is observed. The C_{60}^{+} species produced from $C_{60}H_{22}^{+}$ fragment readily to smaller clusters, while those produced from $C_{66}H_{26}^{+}$ show a mixed fragmentation behavior. As in Figure 2, the vertical dashed lines correspond to the fullerene "magic numbers."

(A color version of this figure is available in the online journal.)

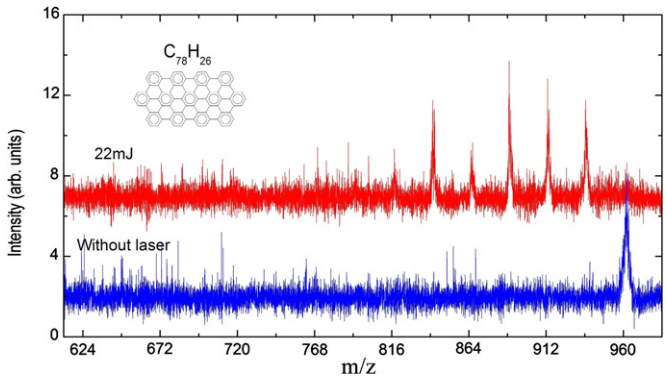

Figure 4. Fragmentation pattern of the fully benzenoid cation, $C_{78}H_{26}^{+}$, irradiated at 355 nm. Note that carbon clusters with 70 C atoms ($m/z = 840$) show enhanced abundances. Due to signal-to-noise limitations, this spectrum was taken at energies lower than those from Figure 2. For this reason fragmentation to lower masses is not achieved.

(A color version of this figure is available in the online journal.)

$C_{78}H_{26}^{+}$ shows an enhanced intensity of the peak corresponding to the C_{70}^{+} carbon cluster, as illustrated in Figure 4.

4. DISCUSSION

The fragmentation pattern of PAHs and fullerenes—specifically the route through C_2 loss from C_{60}—can be quantified through the C_{58}^{+}/C_{60}^{+} ratio. Figure 5 demonstrates the similarity in behavior of the C_{60}^{+} fragments produced from the PAHs and fullerenes at 266 and 355 nm. However, at 532 nm, the C_{60}^{+} fragments produced from $C_{66}H_{26}^{+}$ behave like those produced from C_{70}^{+} (i.e., there is very little fragmentation even at high laser power), while the C_{60}^{+} fragments produced from $C_{60}H_{22}^{+}$ behave similarly to the other wavelengths and fragment readily.

Based on Figures 3 and 5, we conclude that fragmentation of C_{66}^{+} leads to the presence of both non-fullerene C_{60}^{+} isomer(s) as well as the C_{60}^{+} fullerene. We conclude that the loss of C_2 units from the pure carbon cluster, C_{66}^{+}, initiates isomerization of some of the initial fully dehydrogenated PAHs to fullerene cages, which—similar to the C_{70}^{+}—subsequently shrink to smaller and smaller fullerene cages. The results show that this process is very efficient, and a large fraction of the initial clusters (~20% at 85 mJ) are channeled to the C_{60}^{+} fullerene. In contrast, since the isomerization process is initiated by C_2 loss, the C_{60}^{+} fullerene formation channel is essentially closed for

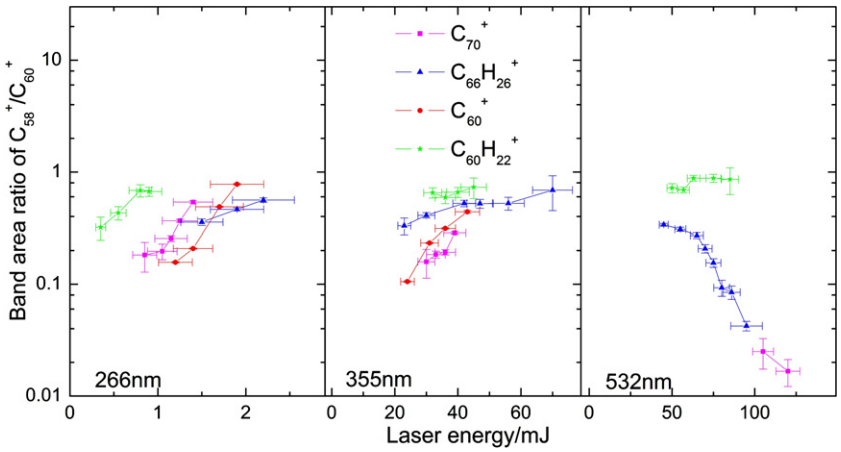

Figure 5. Ratio of the integrated intensity for C_{58}^+/C_{60}^+ as function of laser energy at different wavelengths—266 nm, 355 nm and 532 nm. For the first two wavelengths, the behavior of this ratio for PAH and fullerene cations is very similar. At 532 nm, the behavior of the ratio from $C_{60}H_{22}^+$ deviates from that of the other molecules considered.

(A color version of this figure is available in the online journal.)

the C_{60}^+ produced by dehydrogenating $C_{60}H_{22}^+$ and this species fragments fully to smaller species at 532 nm. We note though that the fragmentation pattern of this PAH for products with $m/z < 720$ resembles that of the fullerenes C_{60} and C_{70}, with peak enhancements at the "magic numbers". Hence, after the C_{60}^+ formed from $C_{60}H_{20}^+$ loses the first C_2, isomerization to cages can be initiated and at this point further fragmentation follows the "cage-route" as well.

Molecular dynamics calculations of the transformation of graphene flakes to fullerenes have revealed that, at high temperatures, this folding process starts through transformation of hexagons at the edges of the flake to various polygons (Lebedeva et al. 2012). Our experiments suggest that the polygon formation associated with this folding process can also be initiated by the loss of C_2 units from the edges of the fully dehydrogenated PAHs and that, once the process is started, it is "self-sustaining" and the chemical energy released quickly drives the complete reconstruction of the dehydrogenated PAH to a fullerene cage.

In summary, we conclude that photofragmentation of PAHs with more than 60 C-atoms leads to the formation of buckminsterfullerene (C_{60}). However, fullerenes are not the only products and isomers with different absorption and stability properties are also formed.

5. ASTROPHYSICAL RELEVANCE

In contrast to our laboratory studies, excitation of PAHs in PDRs is due to single photon absorption. However, irrespective of whether one or multiple photons are involved, rapid intramolecular vibrational redistribution will leave the species highly vibrationally excited from which it relaxes either through fragmentation or IR fluorescence. From our experiments it is not possible to derive the activation energy for the different fragmentation channels and further experiments are needed to confirm if these energies can be reached by single photon absorption in the ISM. In the present study, we will assume that this is the case and, hence, we directly apply our experimental results to the photo-processing of PAHs in space.

Our results provide further insight in the evolution of PAHs in the PDR associated with the reflection nebula NGC 7023. The processes taking place in this nebula are representative for other similar environments in space. In this region, winds from the young Herbig Be star, HD 200775, have blown a cavity in the molecular cloud inside which the star was formed (Fuente et al. 1998). This cavity has broken open to the surrounding ISM. The PAH abundance is observed to decrease—starting at $\sim 25''$ from the star (some $20''$ inside of the PDR front; well within the cavity) from about 7×10^{-2} to 2×10^{-2} of the elemental carbon to about 10^{-2} of the elemental carbon at $10''$ from the star. The fullerene abundance increases from about 10^{-5} at the PDR front to about 10^{-4} some $10''$ from the star (Berné & Tielens 2012).

We can now interpret these observations in terms of the laboratory results presented here and the model described by Berné & Tielens (2012) and Montillaud et al. (2013). The first step in the PAH destruction and fullerene formation process is the loss of peripheral H. H-coverage of PAHs is a balance between UV induced fragmentation and reactions with atomic H and is controlled by the parameter $\gamma = G_0/n_{\rm H}$, where G_0 is the intensity of the UV radiation field in terms of the average interstellar radiation field (Habing 1968) and $n_{\rm H}$ is the atomic hydrogen density in $\rm cm^{-3}$ (Tielens 2005; Le Page et al. 1997). For small γ, a given PAH species will be fully hydrogenated while for large γ, it is fully dehydrogenated and the transition between these two hydrogenation states is very rapid. The critical value of γ separating these two cases is not well known and depends on the PAH size. According to Berné & Tielens (2012), values of $\gamma \approx 3$ and $\gamma \approx 100$ can be calculated for circumcoronene, $C_{54}H_{18}$, and circumovalene, $C_{66}H_{20}$, respectively, based upon kinetic parameters adopted from experimental studies on small PAHs (Jochims et al. 1994; Tielens 2005). Montillaud et al. (2013) on the other hand, adopting slightly different values for the kinetic parameters, predict that for circumcoronene 50% of the species are fully dehydrogenated for $\gamma \approx 4 \times 10^{-2}$ while for circumovalene, this occurs at $\gamma \approx 4 \times 10^{-1}$. Further experimental studies for large PAHs relevant for the ISM will have to settle this issue.

We can compare these values to the γ appropriate for the PDR in NGC 7023. In the cavity of NGC 7023, between $12''$ and $25''$ from the star, where most of the PAH-to-fullerene conversion is observed to occur, γ is estimated to change from 65 to 650 (Berné & Tielens 2012), well into the regime where PAHs in excess of 60 C-atoms will become dehydrogenated. Species that become fully dehydrogenated are rapidly converted into cages but only those initially larger than 60 C-atoms will form C_{60}.

The high stability of C_{60} allows it to accumulate over irradiation time, as can be deduced from Figure 5.

The observed high fraction of PAHs destroyed inside the cavity and the relatively small amount of C_{60} formed in NGC 7023 coupled with the seemingly high efficiency with which large PAHs are converted into the fullerene C_{60} in our experiments suggests then that the population of interstellar PAHs is heavily skewed toward PAHs smaller than 60 C-atoms. The typical size of the interstellar PAH population is not well known. In principle, the ratio of the intensity of the CH stretching mode to the CH out-of-plane bending mode ($I_{3.3\mu m}/I_{11.2\mu m}$) is a measure of the average size of the emitting PAHs (Allamandola et al. 1989; Draine & Li 2001; Ricca et al. 2012). However, the infrared spectrometer on the *Spitzer Space Telescope* did not extend to 3.3 μm while the beam of the Short Wavelength Spectrometer on board of the *Infrared Space Observatory* encompasses the full PDR in NGC 7023. Taking those latter values (Peeters et al. 2002) and a typical excitation energy of 7 eV appropriate for a B3 star ($T_{\rm eff} = 17{,}000$ K), the observed ratio (0.27) translates into an average size of ~60 C-atoms for the emitting PAHs in NGC 7023 (Ricca et al. 2012). Given the beam averaging in these observations, this typical size is likely an overestimate. Furthermore, comparisons of matrix isolation experiments with density functional theory calculations suggest that the latter tends to overestimate the intrinsic strength of the CH stretching mode by a factor of two (Langhoff 1996). Further observational and experimental studies are required to address these issues.

6. CONCLUSION

In agreement with earlier studies, our photofragmentation studies reveal that PAH cations initially fragment through rapid H-loss. The resulting completely dehydrogenated species fragment further through sequential steps of C_2 losses. We compared the results of the fragmentation of the pure carbon clusters formed from PAH cations with those of the fullerenes for different wavelengths.

Using the wavelength dependent absorption cross section properties of C_{60}^+, we demonstrate that PAH fragments formed from PAHs that initially contain more than 60 C-atoms isomerize —among others species— to the fullerene C_{60}. The presence of "magic number" peaks in the fragmentation pattern of smaller PAHs suggests that these isomerize to small cages.

Based on our experimental studies, we have analyzed observational results of PAHs and fullerenes in the NGC 7023 PDR, and conclude that the observed PAH and C_{60} relative abundances imply an interstellar PAH size distribution skewed to sizes $\lesssim$60 C-atoms. These experiments provide direct support for the importance of top-down photochemistry for the formation of fullerenes in the ISM, as well as other species. However, it must be noted that further experiments are needed to determine the relevant fragmentation energies and the feasibility that photons with these energies are available in the ISM.

Finally, we recognize that, in a laboratory setting, the efficient complete dehydrogenation of PAHs provides a novel way to synthesize pure carbon clusters (most likely graphene flakes) of very specific sizes. Given the present interest in graphene, this synthesis method holds much potential for the study of such species under fully controlled conditions and will allow a validation of theoretically predicted properties by experiments.

We are grateful to M.J.A. Witlox and R. Koehler for technical support. We are grateful to L.J. Allamandola who provided the large PAH sample. Studies of interstellar chemistry at Leiden Observatory are supported through advanced-ERC grant 246976 from the European Research Council, through a grant by the Dutch Science Agency, NWO, as part of the Dutch Astrochemistry Network, and through the Spinoza premie from the Dutch Science Agency, NWO.

REFERENCES

Allamandola, L. J., Tielens, A. G.G. M., & Barker, J. R. 1989, ApJS, 71, 733
Becker, L., Bada, J. L., Winans, R. E., & Bunch, T. E. 1994, Natur, 372, 507
Berné, O., & Tielens, A. G.G. M. 2012, PNAS, 109, 401
Cami, J., Bernard-Salas, J., Peeters, E., & Malek, S. E. 2010, Sci, 329, 1180
Candian, A., Sarre, P. J., & Tielens, A. G.G. M. 2014, ApJL, 791, L10
Castellanos, P., Berné, O., Sheffer, Y., Wolfire, M., & Tielens, A. G.G. M. 2014, ApJ, 794, 83
Cherchneff, I., Barker, J. R., & Tielens, A. G.G. M. 1992, ApJ, 401, 269
Chuvilin, A., Kaiser, U., Bichoutskaia, E., Besley, N. A., & Khlobystov, A. N. 2010, NatCh, 2, 450
Doucet, C., Habart, E., Pantin, E., et al. 2007, A&A, 470, 625
Draine, B. T., & Li, A. 2001, ApJ, 551, 807
Ekern, S. P., Marshall, A. G., Szczepanski, J., & Vala, M. 1998, JPCA, 102, 3498
Frenklach, M., & Feigelson, M. E. 1989, ApJ, 341, 372
Fuente, A., Martin-Pintado, J., Rodriguez-Franco, A., & Moriarty-Schieven, G. D. 1998, A&A, 339, 575
Habart, E., Natta, A., Testi, L., & Carbillet, M. 2006, A&A, 449, 1067
Habing, H. J. 1968, BAN, 19, 421
Handschuh, H., Gantefor, G., Kessler, B., Bechthold, P. S., & Eberhardt, W. 1995, PhRvL, 74, 1095
Herbst, E., & van Dishoeck, E. F. 2009, ARA&A, 47, 427
Hollenbach, D. J., & Tielens, A. G.G. M. 1999, RvMP, 71, 173
Joblin, C. 2003, in SF2A-2003: Semaine de l'Astrophysique Française, ed. F. Combes, D. Barret, T. Contini, & L. Pagani (Lesulis, France: EDP Sciences), 175
Jochims, H. W., Ruhl, E., Baumgartel, H., Tobita, S., & Leach, S. 1994, ApJ, 420, 307
Koskinen, P., Malola, S., & Häkkinen, H. 2008, PhRvL, 101, 115502
Langhoff, S. R. 1996, JPhCh, 100, 2819
Lebedeva, I. V., Knizhnik, A. A., Popov, A. M., & Potapkin, B. V. 2012, JPCC, 116, 6572
Le Page, V., Keheyan, Y., Bierbaum, V. M., & Snow, T. P. 1997, JACS, 119, 8373
Lifshitz, C. 2000, IJMS, 200, 423
Malloci, G., Joblin, C., & Mulas, G. 2007, CP, 332, 353
McEwan, M. J., Scott, G. B.I., Adams, N. G., et al. 1999, ApJ, 513, 287
Montillaud, J., Joblin, C., & Toublanc, D. 2013, A&A, 552, A15
Peeters, E., Hony, S., Van Kerckhoven, C., et al. 2002, A&A, 390, 1089
Pety, J., Teyssier, D., Fossé, D., et al. 2005, A&A, 435, 885
Poater, J., Visser, R., Solà, M., & Bickelhaupt, F. M. 2007, JOC, 72, 1134
Rapacioli, M., Joblin, C., & Boissel, P. 2005, A&A, 429, 193
Ricca, A., Bauschlicher, C. W., Jr., Boersma, C., Tielens, A. G.G. M., & Allamandola, L. J. 2012, ApJ, 754, 75
Sellgren, K., Wener, M. W., Ingalls, J. G., et al. 2010, ApJ, 722, 54
Sephton, M. A., & Botta, O. 2008, SSRv, 135, 25
Tatsuhisa, K., Takeshi, K., Tadamasa, S., et al. 1991, CPL, 180, 446
Tielens, A. G.G. M. 2005, The Physics and Chemistry of the Interstellar Medium (1st ed.; Cambridge: Cambridge Univ. Press)
Tielens, A. G.G. M. 2008, ARA&A, 46, 289
Tielens, A. G.G. M. 2013, RvMP, 85, 1021
Zhen, J., Paardekooper, D. M., Candian, A., Linnartz, H., & Tielens, A. G.G. M. 2014, CPL, 592, 211
Zimmerman, J. A., Eyler, J. R., Bach, S. B.H., & McElvany, S. W. 1991, JCP, 94, 3556